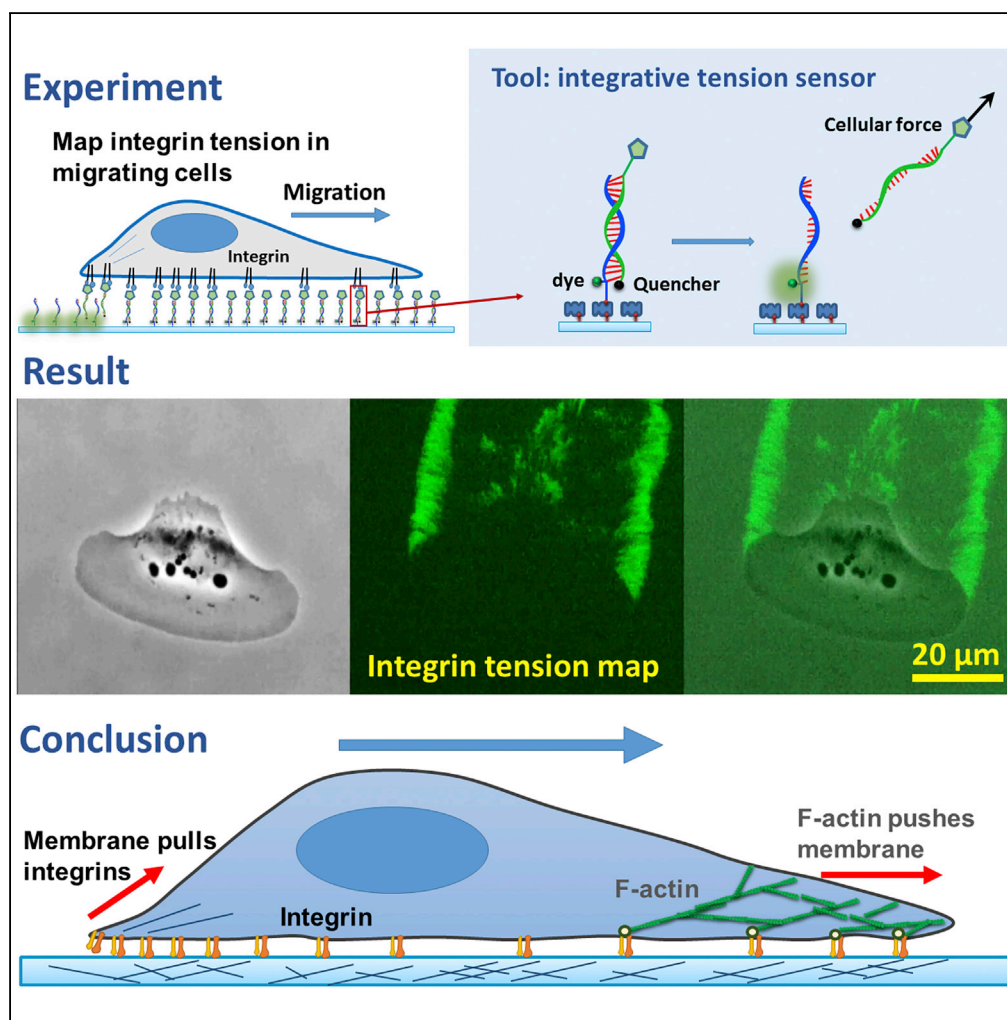


## Article

# Keratocytes Generate High Integrin Tension at the Trailing Edge to Mediate Rear De-adhesion during Rapid Cell Migration



Yuanchang Zhao,  
Yongliang Wang,  
Anwasha Sarkar,  
Xuefeng Wang

xuefeng@iastate.edu

### HIGHLIGHTS

Tension sensor (ITS) mapped and calibrated integrin tension in migratory cells

High-level integrin tension (HIT) above 54 pN was observed in migrating keratocytes

HIT is exclusively and narrowly localized at the cell rear margin

HIT peels off focal adhesions at cell rear and facilitates keratocyte retraction

Zhao et al., iScience 9, 502–512  
November 30, 2018 © 2018  
The Author(s).  
<https://doi.org/10.1016/j.isci.2018.11.016>

## Article

# Keratocytes Generate High Integrin Tension at the Trailing Edge to Mediate Rear De-adhesion during Rapid Cell Migration

Yuanchang Zhao,<sup>1</sup> Yongliang Wang,<sup>1</sup> Anwesha Sarkar,<sup>1</sup> and Xuefeng Wang<sup>1,2,3,\*</sup>**SUMMARY**

Rapid cell migration requires efficient rear de-adhesion. It remains undetermined whether cells mechanically detach or biochemically disassemble integrin-mediated rear adhesion sites in highly motile cells such as keratocytes. Using molecular tension sensor, we calibrated and mapped integrin tension in migrating keratocytes. Our experiments revealed that high-level integrin tension abbreviated as HIT, in the range of 50–100 pN (piconewton) and capable of rupturing integrin-ligand bonds, is exclusively and narrowly generated at cell rear margin during cell migration. Co-imaging of HIT and focal adhesions (FAs) shows that HIT is produced to mechanically peel off FAs that lag behind, and HIT intensity is correlated with the local cell retraction rate. High-level molecular tension was also consistently generated at the cell margin during artificially induced cell front retraction and during keratocyte migration mediated by biotin-streptavidin bonds. Collectively, these experiments provide direct evidence showing that migrating keratocytes concentrate force at the cell rear margin to mediate rear de-adhesion.

**INTRODUCTION**

Eukaryotic cell migration is crucially important for immunity (Luster et al., 2005), development (Weijer, 2009), wound healing (Poujade et al., 2007) and many other physiological processes (Lamallice et al., 2007; Yilmaz and Christofori, 2010). Cellular force plays a pivotal role to drive and regulate cell migration (Huttenlocher and Horwitz, 2011; Sheetz et al., 1998), which is typically orchestrated by two critical motion modules: cell protrusion in the leading edge and de-adhesion in the trailing edge (Gardel et al., 2010; Pollard and Borisy, 2003). The cellular force mediating cell protrusion has been well studied and understood. Actin network polymerizes in the cell leading edge and pushes the cell membrane forward, thus advancing the cell front edge (Le Clainche and Carlier, 2008; Theriot and Mitchison, 1991). In contrast, how cells detach the rear adhesion sites in the trailing edge is not fully understood. During cell migration, the adhering integrins in the cell rear region need be efficiently detached from the surface ligands to facilitate cell migration. Previously it was suggested that cells may biochemically regulate integrin de-adhesion in less motile cells (Franco and Huttenlocher, 2005). For example, protein calpain has been shown to mediate the release of cell-substrate adhesion during fibroblast migration (Palecek et al., 1998; Undyala et al., 2008). However, biochemical regulation of cell de-adhesion may not be efficient in highly motile cells such as keratocytes, which are capable of migrating at a rate higher than 10  $\mu\text{m}/\text{min}$  (Maiuri et al., 2012). A plausible mechanism of cell rear de-adhesion with higher efficiency could be mechanical dissociation of integrin-ligand bonds by cellular force at the cell rear, as mechanical signals propagate faster than biochemical signals in cells (Houk et al., 2012). In this mechanism, cells may produce high integrin tension at the level of integrin-ligand bond strength at the cell trailing edge to mechanically break integrin-ligand bonds and facilitate cell rear de-adhesion and migration. Therefore, measuring and mapping integrin tension in migrating cells would yield important insights to the mechanism of cell migration. Integrin tension has been calibrated in stationary or low motile cells (Galior et al., 2016; Liu et al., 2013, 2014; Wang et al., 2015; Wang and Wang, 2016). However, before this work, no experiments have calibrated or mapped integrin tension in fast migrating cells.

Here we applied integrative tension sensor (ITS) to calibrate and map integrin tension in migrating cells with submicron resolution and high sensitivity. ITS was previously developed to map integrin tension in platelets (Wang et al., 2017). By converting integrin tension above a designed threshold to fluorescent signal, ITS enables integrin tension mapping directly by fluorescence imaging. Using ITS, here we calibrated and mapped integrin tension in fish epidermal keratocytes, which are classic cell models for the study of rapid cell migration in a crawling mode. Our experiments revealed that migrating keratocytes

<sup>1</sup>Department of Physics and Astronomy, Iowa State University, 12 Physics Hall, Ames, IA 50011, USA

<sup>2</sup>Molecular, Cellular, and Developmental Biology Interdepartmental Program, Molecular Biology Building, Ames, IA 50011, USA

<sup>3</sup>Lead Contact

\*Correspondence: xuefeng@iastate.edu

<https://doi.org/10.1016/j.isci.2018.11.016>



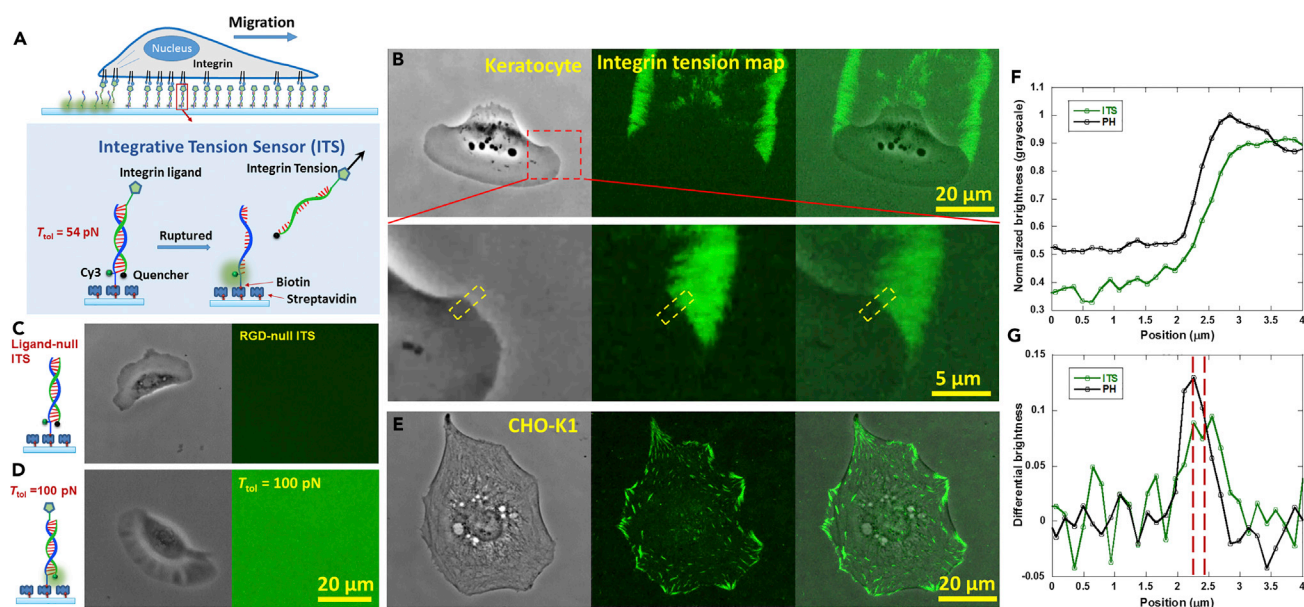


**Figure 1. High-Level Integrin Tension (HIT) Is Exclusively Generated at Cell Rear Margin in Migrating Keratocytes**

(A) Schematics of integrative tension sensor (ITS). ITS is a surface-immobilized 18-bp dsDNA labeled by an integrin ligand and a fluorophore-quencher pair. ITS permanently turns to fluoresce if the tension transmitted by integrin-ligand bond ruptures the dsDNA, which has a tension tolerance ( $T_{tol}$ ) of 54 pN. (B) Integrin tension (>54 pN) of a migrating keratocyte was mapped on the ITS surface by fluorescence imaging. Refer to [Video S1](#). (C) Keratocytes produced no signal on the ligand-null ITS surface. (D) Keratocytes produced no fluorescence loss on the quencher-null ITS with  $T_{tol}$  determined by biotin-streptavidin bond strength (the ligand and the biotin are conjugated to the same strand). (E) Integrin tension (>54 pN) of a stationary CHO-K1 cell was mapped on the ITS surface. (F) Linear profile analysis of the image brightness in the regions marked by yellow dashed lines in (B). The sharp brightness increases in phase contrast (PH) and Cy3 (ITS) channels mark the cell margin and the active site of integrin tension generation, respectively. (G) Cell margin and ITS border represented by the peaks of derivative curves of linear profiles in (F). The peak locations are marked by red dashed lines.

generate integrin tension in the range of 50–100 pN exclusively at the cell rear margin to rupture the local integrin-ligand bonds, peel off focal adhesions (FAs), and mediate cell de-adhesion.

## RESULTS

### Mapping Integrin Tension in Migrating Keratocytes Using Molecular Tension Sensor

Using ITS, we mapped integrin molecular tension in migrating keratocytes. ITS was previously developed in our laboratory to study platelet force during adhesion and contraction (Wang and Ha, 2013; Wang et al., 2017). ITS converts molecular tension signal to fluorescence on site, thus enabling integrin tension mapping directly by fluorescence imaging. Briefly, as shown in [Figure 1A](#), ITS is an 18 base-paired (bp) double-stranded DNA (dsDNA) decorated with a fluorophore Cy3, a quencher (BHQ2, black hole quencher), a biotin tag, and an integrin peptide ligand RGD (Arginine-glycine-aspartic acid), which targets a broad range of integrins, such as integrins  $\alpha_v\beta_3$ ,  $\alpha_{IIb}\beta_3$ , and  $\alpha_5\beta_1$  (Mondal et al., 2013). The BHQ2 quencher efficiently suppresses fluorescence of the Cy3 with 96.6% quenching efficiency ([Figure S1](#)), close to 98% contact quenching (Crisalli and Kool, 2011). On a surface grafted with ITS, integrin of adherent cells binds to the integrin ligand and transmits a tension to the dsDNA through the integrin-ligand bond. If the tension is higher than the tension tolerance of the dsDNA ( $T_{tol}$ , critical force required for dsDNA dissociation with force application time in seconds, tunable in the range of 12–54 pN) (Wang and Ha, 2013), the dsDNA will be dissociated and the Cy3 will be freed from quenching, thus converting tension signal to fluorescent signal *in situ* (Wang et al., 2017). ITS activation is irreversible and therefore records all dsDNA-dissociating integrin tensions on the surface. This signal accumulation process greatly enhances the sensitivity for integrin tension mapping. This is particularly important for the study of migrating cells in which cellular force is transient and constantly changing.

In this paper, we studied integrin tension at a high level in keratocytes using ITS at  $T_{tol} = 54$  pN, which is the critical force to rupture 18-bp dsDNA in a shear geometry with a force dwell time of 2 s (Hatch et al., 2008).

ITS is immobilized on a glass surface by biotin-streptavidin interaction. The dsDNA in the ITS has undetectable spontaneous dissociation in the time span of the experiments (1–2 hr) at room temperature (25°C), suggesting that the ITS is thermally stable. The surface coating is also doped with fibronectin to assist cell adhesion and minimize the influence of ITS rupture to cell normal migration. Keratocytes were plated on the ITS surface. At room temperature, most keratocytes polarized and migrated normally in about 15 min. Strong fluorescence signal was produced by migrating keratocytes on the ITS surface (Figure 1B and Video S1). Hence, integrin tension stronger than 54 pN in keratocytes was directly mapped by fluorescence imaging. To confirm that the fluorescence signal was indeed activated by integrin tension, we plated keratocytes on a surface coated with ligand-null ITS, which has no integrin ligand. Migrating keratocytes produced no fluorescence signal on the ligand-null ITS surface (Figure 1C), confirming that the fluorescence on the regular ITS surface was activated by integrin tension. The integrins transmitting high tensions are likely to be integrin  $\alpha_5\beta_1$  or  $\alpha_v\beta_3$  as demonstrated by previous research (Riaz et al., 2016). To determine the upper limit of integrin tension in keratocytes, we prepared another construct of ITS in which integrin ligand and biotin are conjugated to the same single-stranded DNA (ssDNA) at two ends (Figure 1D). The  $T_{tol}$  of this ITS construct is determined by biotin-streptavidin bond strength, which was calibrated to be around 100 pN with force dwell time of seconds (Pincet and Husson, 2005). The complementary ssDNA is conjugated with Cy3 dye. Integrin tension capable of rupturing biotin-streptavidin bonds would remove Cy3 dyes from the surface and cause local fluorescence loss. However, keratocytes left no detectable fluorescence signal on the biotin-streptavidin-based ITS surface, indicating that the integrin tension generated by migrating keratocytes is generally lower than the bond strength of biotin-streptavidin.

### Integrin Tension Is Exclusively and Narrowly Generated at Cell Rear Margin in Migrating Cells

Using ITS with  $T_{tol} = 54$  pN, we mapped the high-level integrin tension (HIT) in migrating keratocytes. The most striking feature of HIT map in migrating keratocytes is that the HIT is exclusively and narrowly generated at the cell rear margin (Figure 1B and Video S1). The cell rear margin shown by phase-contrast (PH) imaging consistently overlaps with the border of HIT regions during the entire process of keratocyte migration. On the contrary, in stationary CHO-K1 cells, HIT is globally generated underneath the cell bodies without being restricted to the cell margin (Figure 1E). Line profile analysis over the region marked by yellow lines in Figure 1B were calculated and plotted in Figure 1F. The cell margin and the border of HIT map reported by the sharp brightness increases in the two curves clearly overlap with each other. To better confirm their co-localization, we computed the derivatives of the two curves in Figure 1F and plotted them in Figure 1G. The peaks of derivative curves marking the cell margin and the border of activated ITS regions, respectively, is co-localized with each other with a precision of 0.5  $\mu\text{m}$ . This narrow co-localization verifies that HIT is generated at the cell rear margin within a submicron margin width, suggesting that HIT is highly concentrated at the cell trailing edge.

### HIT Is in Range of 50–100 pN

The critical forces to rupture a dsDNA and a biotin-streptavidin bond are both dependent on the force dwell time. To use the  $T_{tol}$  value of ITS to evaluate integrin tension, the dwell time of integrin tension must be in the same range of the ITS calibration time. Based on the narrow sites for HIT generation, we estimated the dwell time of HIT at the keratocyte rear margin. Because the cell migration rate is 10–20  $\mu\text{m}/\text{min}$  and the width of HIT generation is around 1  $\mu\text{m}$  (the width of the slope of ITS curve in Figure 1F), the cell edge should sweep through the HIT region in less than 10 s. Therefore, the dwell time of integrin tension at the cell rear margin should be in the range of seconds, matching the force dwell time ranges used for the  $T_{tol}$  calibrations of dsDNA (Hatch et al., 2008) in the 54-pN ITS and biotin-streptavidin bond (Pincet and Husson, 2005) in the 100-pN ITS. Therefore, it is valid to use these  $T_{tol}$  values to evaluate the integrin tension range in keratocytes. We conclude that HIT is in the range of 50–100 pN during keratocyte migration.

### HIT Is Capable of Rupturing Integrin-Ligand Bonds

Keratocytes produce integrin tension that readily ruptures 18-bp dsDNA. We reasoned that such tension is produced to break integrin-ligand bonds at the cell trailing edge to facilitate cell rear de-adhesion. This is supported by two lines of evidence. First, integrin-ligand bond strength was calibrated to be in the range of 30–40 pN with force application time of seconds in a previous study (Kong et al., 2009). The bond strength is at a level comparable with the 54 pN  $T_{tol}$  of ITS. Therefore, the HIT reported by ITS should be capable of rupturing integrin-ligand bond with a high probability. Second, we enhanced integrin-ligand bond strength by adding 2 mM  $\text{Mn}^{2+}$  (Kong et al., 2009) in the medium (Figure 2A, Video S2), and the ITS signal

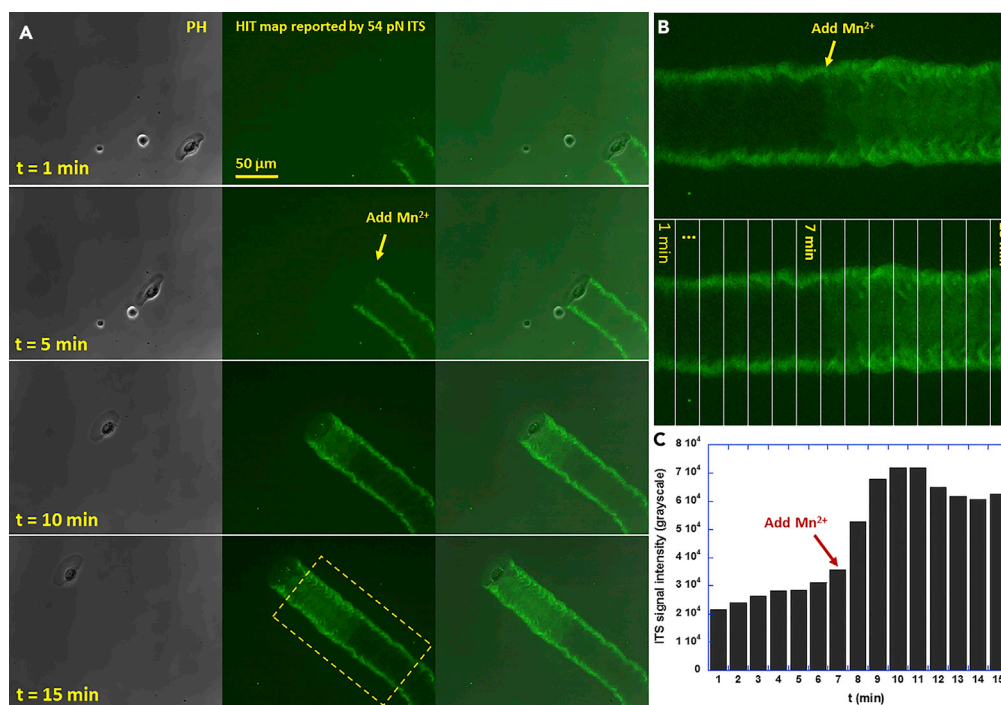


### Figure 2. Enhancing Integrin-Ligand Bond Strength with 2 mM Mn<sup>2+</sup> Led to Stronger ITS Signal

(A) Time-series HIT maps of a migrating keratocyte. At  $t = 7$  min after starting imaging, 2 mM Mn<sup>2+</sup> was added to the cell medium. The images were processed based on [Video S2](#).

(B) HIT map segmentation by time. This map region was processed from the area of [Figure 2A](#) marked by yellow dashed line.

(C) ITS signal intensity analysis. The ITS signal was immediately increased by 2 mM Mn<sup>2+</sup> by 2.5-fold, suggesting that integrin-ligand bond dissociation is in company with ITS activation under normal physiological condition, and ITS signal can report the location where integrin-ligand bonds are mechanically dissociated. The ITS signal was calculated by averaging the grayscale values of pixels in the rectangular grids in [Figure 2B](#).

was immediately increased by 2.5-fold in a migrating keratocyte ([Figures 2B](#) and [2C](#)), suggesting that considerable amount of integrin-ligand bonds were ruptured in company with ITS activation under normal physiological condition if without the addition of Mn<sup>2+</sup>. Therefore, we inferred that keratocytes generate integrin tension at the level of integrin-ligand bond strength during migration, and the 54-pN ITS signal reports the location where integrin-ligand bonds are mechanically dissociated by cells. "High-level integrin tension" (HIT) in the following context specifically refers to the tension reported by ITS with  $T_{\text{tol}} = 54$  pN that is capable of rupturing integrin-ligand bonds under normal physiological condition.

### HIT Peels off Focal Adhesions Lagging behind at the Cell Rear Margin

ITS enables the simultaneous imaging of cellular force and cellular structure at submicron resolution. Because integrin clusters called FAs are the main adhesion complexes mediating cell adhesion ([Carragher and Frame, 2004](#)), we speculate that HIT may be generated at the cell rear margin to mechanically detach FAs during cell migration. Here we analyzed the co-localization of HIT and FAs in keratocytes by fixing keratocytes on an ITS surface and immunostaining vinculin, which marks FAs. Imaging shows that HIT regions indeed share borders with the two large FAs at the two rear flank sites of a keratocyte ([Figure 3A](#)). However, despite the large area of the two FAs, only the edges of the FAs coinciding with the cell margin transmit HIT, as shown by the margin analysis of FA, phase contrast, and ITS images in [Figure 3B](#). This result suggests that keratocytes generate HIT on integrin-ligand bonds at the edge of FAs and peel FAs off from the surface to facilitate cell retraction and migration.

Next, we examined the co-localization of actomyosin and HIT. Actomyosin is the protein complex of myosin II and F-actin, which is an important force source for cell contractility ([Murrell et al., 2015](#)) and fibroblast motility ([Even-Ram et al., 2007](#)). Previous studies show that actomyosin produces integrin tensions in

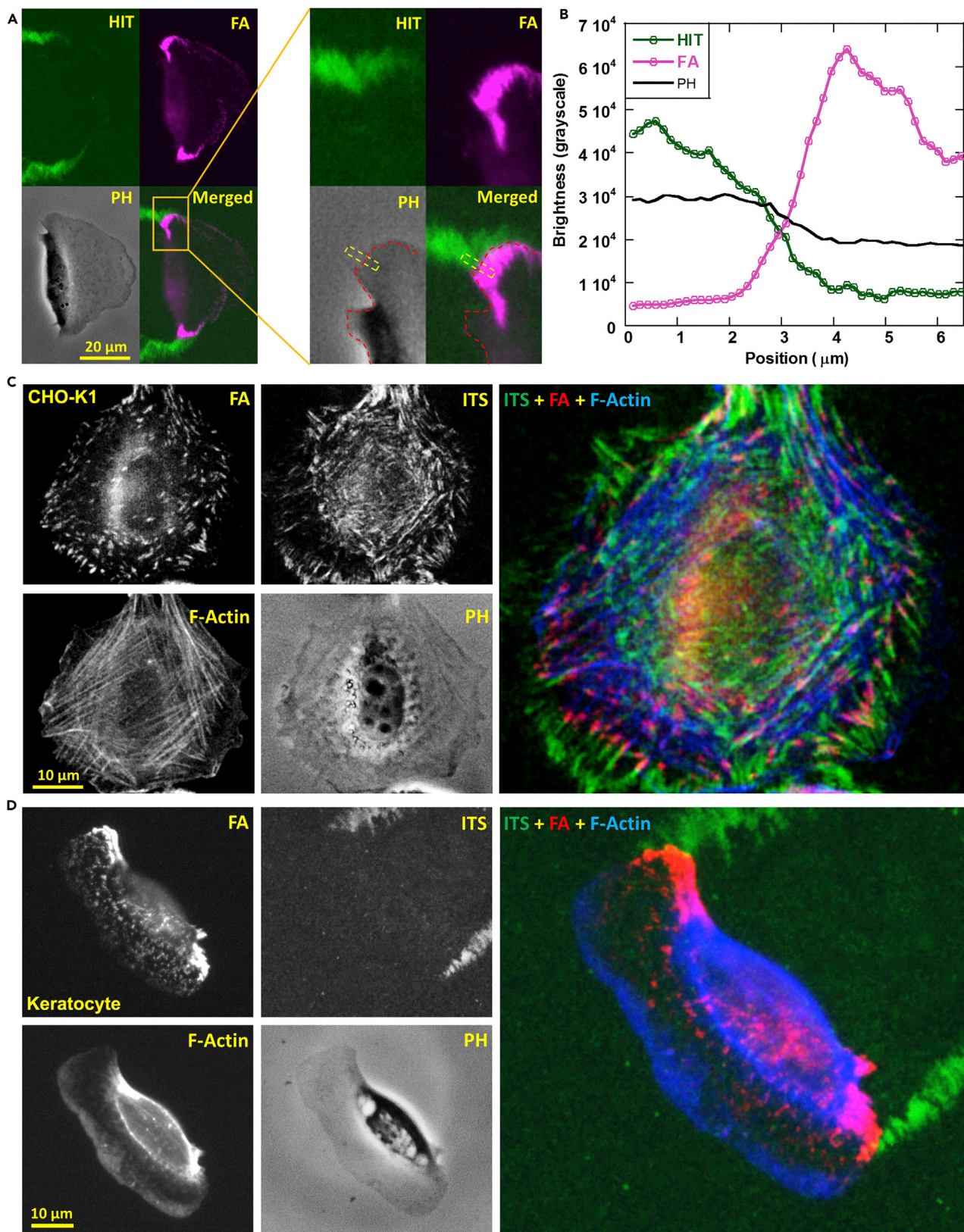


**Figure 3. HIT Occurs at the Edge of Focal Adhesions (FAs) Coinciding with Cell Rear Margin**

- (A) Co-imaging of HIT map, phase contrast (PH), and FAs immunostained with vinculin antibody.
- (B) Line profiles of HIT, FA, and phase contrast imaging in the rectangular region marked by the yellow dashed line in (A), showing that HIT map, FAs, and the cell margin share a thin border, and only integrins at the edges of FAs coinciding with membrane margin transmit HIT.
- (C) Co-imaging of HIT and cellular structures, including FAs, F-actin, and cell membrane, in a CHO-K1 cell. HIT was produced in most FAs underneath cells.
- (D) Co-imaging of HIT and cell structures in a keratocyte. HIT was exclusively produced at the cell rear margin.

FAs in cells with low motility, such as HCC 1143 cells (Jurchenko et al., 2014) and CHO-K1 cells (Wang et al., 2015). Actomyosin is visible by F-actin staining and usually identified as stress fibers in cells. As a control experiment, we co-imaged FAs, stress fibers, and HIT in stationary CHO-K1 cells. The HIT signals are broadly distributed underneath the CHO-K1 cell body, not limited to the cell membrane margin (Figure 3C). The merged images of FA, stress fibers, and ITS signals in Figures 3C and S2 show that each FA is linked to a stress fiber and activates ITS signals under the cell body, suggesting that stress fibers likely generate traction forces on FAs and produce HIT in FAs in CHO-K1 cells, consistent with previous study showing that actomyosin is the force source of HIT in less motile cells (Wang et al., 2015). However, in migrating keratocytes, despite that numerous FAs and stress fibers form in the cell (Figure 3D), none of FAs underneath the cell body generated HIT. The stress fibers have no spatial connection with HIT signals either. HIT is exclusively located on the cell rear margin at the cell trailing edge, suggesting that actomyosin does not correlate with the generation of HIT in migrating keratocytes.

**HIT Signal Intensity Correlates Locally with Cell Rear Retraction**

To investigate the role of HIT in cell migration, we studied the correlation between real-time HIT signal and membrane rear retraction. Real-time HIT was acquired by subtracting the previous frame from a current frame of an ITS video. This frame subtraction method obtains HIT produced in the latest frame interval and can be approximately treated as real-time HIT signal. Figure 4A shows time-series images of real-time HIT map by frame subtraction method (frame interval: 20s, Video S3). The real-time integrin tension activity is compared with cell membrane retraction intensity (defined as the square of local membrane retraction distance at integrin tension regions) during that frame interval. Membrane retraction is illustrated in the second column of Figure 4A, in which cell contours at the current frame (green) and the previous frame (magenta) were drawn to show the movement of keratocytes. The real-time HIT regions are well sandwiched between the two cell contours at the cell rear. Real-time HIT signal intensity correlates with local membrane retraction intensity with a correlation coefficient of 0.87 (Figure 4B), suggesting that HIT is likely generated to assist cell rear de-adhesion and retraction. Interestingly, real-time HIT intensity per frame has a large variation and exhibits a period of about 2 min in the cell (Figure 4C), reminiscent to the periodic stretching of keratocyte membrane observed in previous studies (Barnhart et al., 2010; Lee et al., 1999).

**HIT Was Consistently Generated at the Cell Margin during Acutely Induced Membrane Retraction**

During normal keratocyte migration, HIT is generated to peel off rear FAs and facilitate cell retraction. To verify that HIT is consistently required to mediate cell de-adhesion and retraction, here we induced cell retraction at other regions including the cell front using hypertonic medium that acutely reduces cell volume and causes cellular shrinkage (Weyand et al., 1998). In experiments, cell culture medium spiked with 150 mM sucrose was added to migrating keratocytes on a 54-pN ITS surface. Imaging was performed on cells in the next 5 min immediately after the medium exchange. The HIT map is displayed in green and the real-time HIT gained in the latest frame interval (10 s) is in red in Figures 5A and 5B. Within 1 min after medium exchange, irregular cell membrane retraction started to occur in all cell peripheral regions, including the lateral sides and the cell front edge (shown by orange arrows in Figure 5A and Video S4). During the induced cell retraction, HIT signal was consistently and narrowly produced at the cell margin at all retraction sites, including cell front retraction. The real-time HIT signal during the induced cell retraction is typically located at the cell margin with a width less than 0.5  $\mu\text{m}$  (Figure S3), being consistent with the fact that HIT is narrowly generated at the retracting cell margin in normal keratocyte migration.

**ITS Signal Was Generated at Cell Rear Margin in Biotinylated Keratocytes That Migrate via Biotin-Streptavidin Bonds**

We further investigate whether HIT is a general approach for cell de-adhesion and retraction in migrating keratocytes. An experiment was designed to test integrin-independent keratocyte migration. We

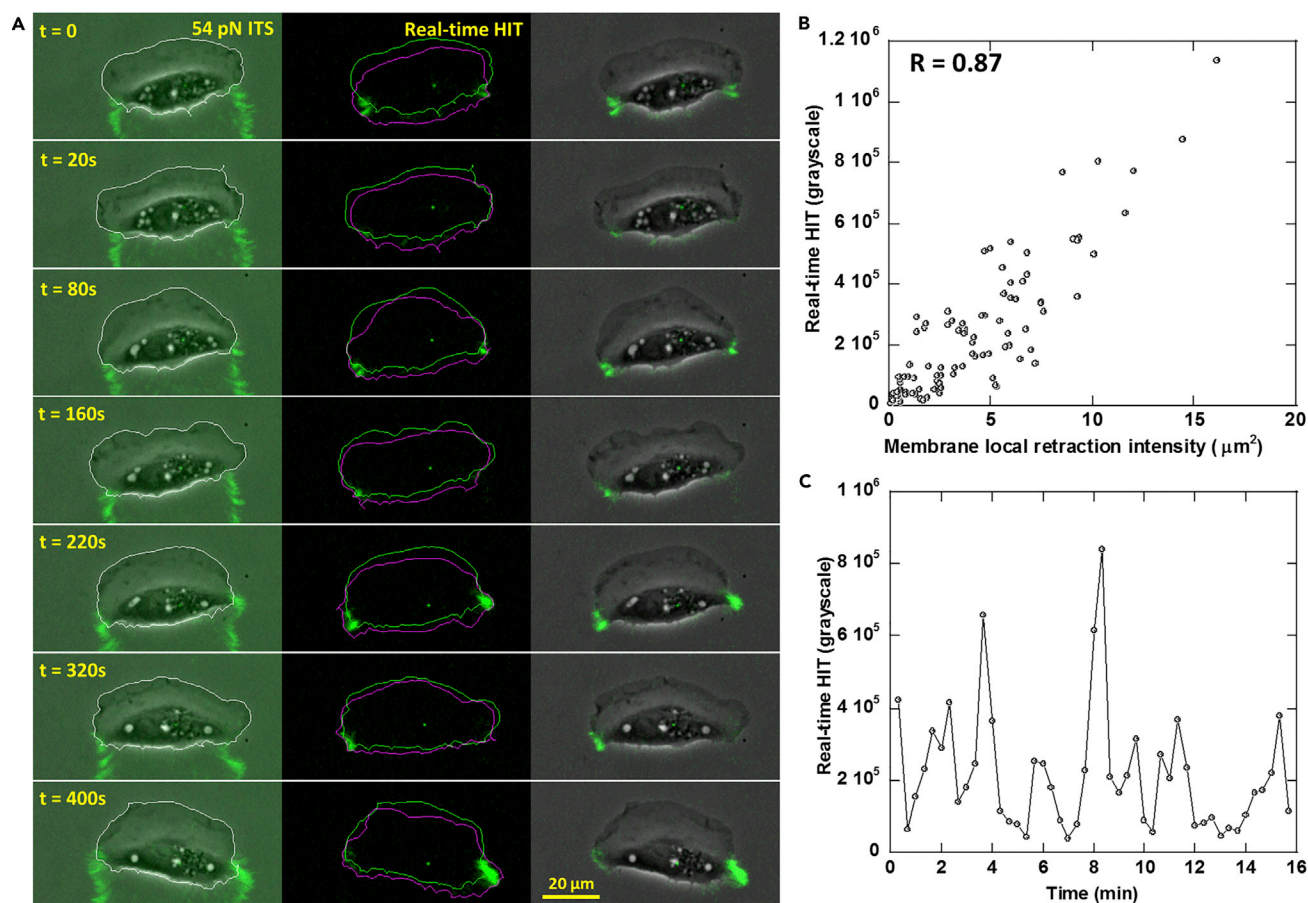


**Figure 4. Correlation between Real-Time HIT Intensity and Cell Membrane Retraction**

(A) Time-lapse ITS imaging ( $T_{\text{tot}} = 54$  pN). The second column shows the cell membrane contours in two consecutive imaging frames with a frame interval of 20 s. Green contour is for the cell in current frame, and magenta contour is for the cell in the previous frame. Real-time HIT marked by ITS signal gain (green) was acquired by subtracting the previous frame from a current frame of ITS imaging. Real-time HIT represents the integrin tension signals produced in the latest 20 s. Refer to [Video S3](#).

(B) A scatterplot of the local real-time HIT intensity and the corresponding membrane retraction intensity (defined as the square of local membrane retraction distance at the ITS signal region).

(C) Real-time HIT intensity versus time.

biotinylated membrane proteins of keratocytes and tested keratocyte migration based on biotin-streptavidin-mediated adhesion instead of integrin-mediated adhesion. Keratocytes re-suspended in serum-free medium were treated with NHS ester-labeled biotin. The NHS ester readily reacts with amine group in the membrane proteins of keratocytes and covalently labels the proteins with biotins. The biotinylated keratocytes are able to adhere on streptavidin surfaces without integrin ligands. A new construct of ITS ([Figure 5C](#)) was designed to map the tension transmitted by biotin-streptavidin bonds. The ITS was covalently conjugated with BSA, which enables ITS surface immobilization by physical adsorption. The other end of the ITS has a biotin tag to immobilize streptavidin. Biotinylated keratocytes were plated on the ITS-coupled streptavidin surfaces. The keratocytes were shown to adhere and migrate normally on the surface. ITS signal was also generated by the migrating keratocytes on the surface ([Figure 5D](#) and [Video S5](#)). Instead of the typical two-track force map due to the peeling of the large FAs at two sides in regular keratocytes, biotinylated keratocytes generated nearly homogeneous ITS signal behind the cells. This is likely because the membrane proteins are relatively uniformly distributed on the cell membrane and biotin-streptavidin interaction occurs evenly under the cells. Remarkably, the ITS signal transmitted by the biotin-streptavidin bonds is still exclusively generated at the cell rear margin ([Figure 5E](#)), demonstrating that keratocytes have the ability to concentrate force at cell rear to mechanically peel off rear adhesion sites and facilitate cell migration even in an integrin-independent manner.

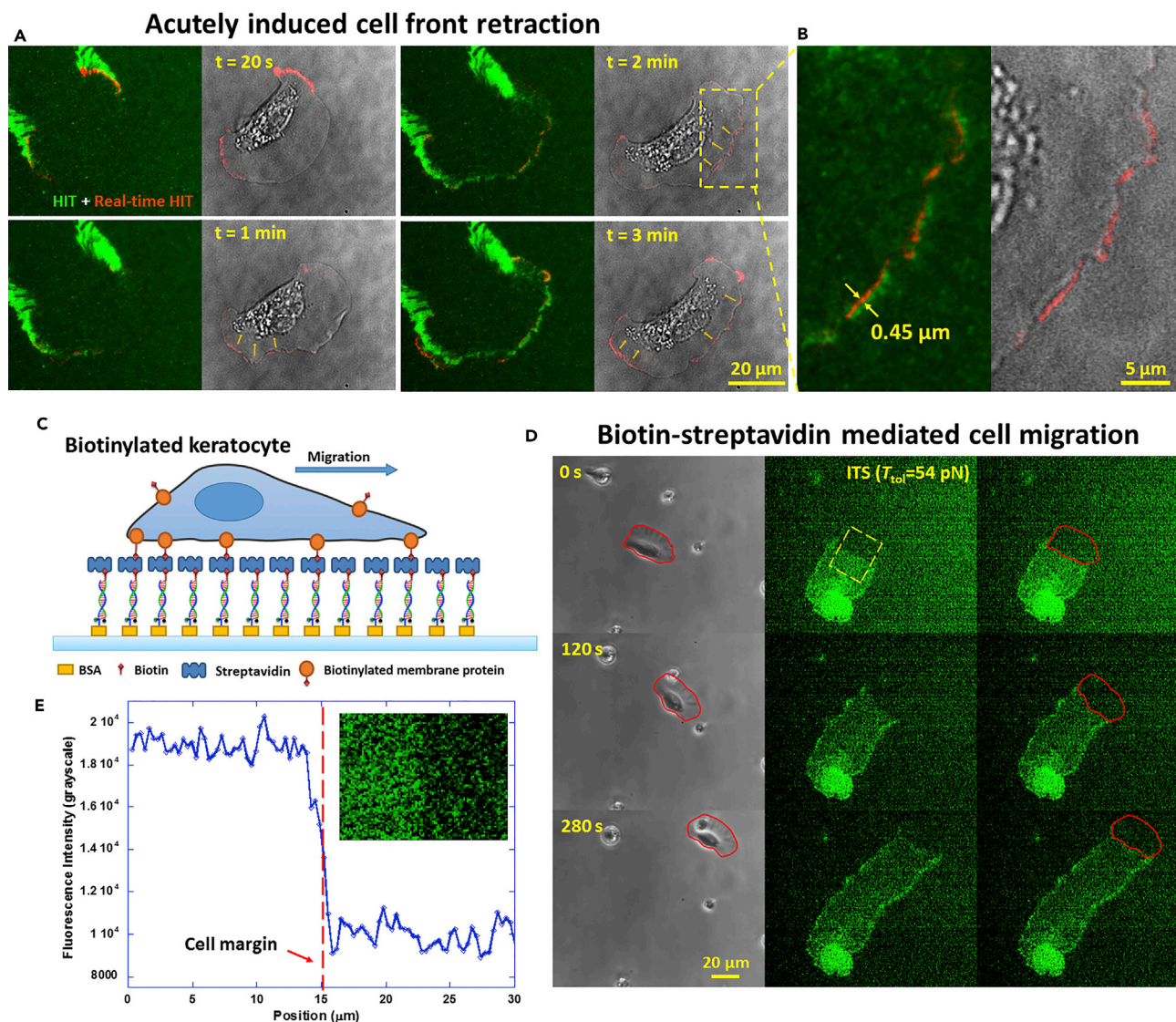


**Figure 5. ITS Signal during Acutely Induced Cell Front Retraction and Biotin-Streptavidin Bond-Mediated Keratocyte Migration, Respectively**

(A) Time-series of HIT maps in keratocytes after a treatment with hypertonic medium (cell culture medium spiked with 150 mM sucrose). HIT signal is colored in green, and real-time HIT (HIT gained in the latest 10 s) is colored in red. Hypertonic medium was added at  $t = 0$  s. The induced local cell membrane retraction sites are marked by orange arrows. Refer to [Video S4](#).

(B) Zoom-in images of HIT map and the cell membrane. The width of real-time HIT region is  $0.45 \mu\text{m}$ .

(C) Cell membrane proteins of keratocytes were biotinylated. Keratocytes adhered and migrated by biotin-streptavidin interaction instead of integrin-ligand binding. Molecular tension transmitted by biotin-streptavidin bonds during keratocyte migration was recorded by modified ITS that is conjugated to BSA and immobilized on the surface by physical adsorption.

(D) Time-lapse images of a keratocyte that migrated via biotin-streptavidin bonds. ITS signal was consistently generated at the cell rear margin during this integrin-independent cell migration. Refer to [Video S5](#).

(E) Co-localization analysis of cell margin and tension map indicates that tension transmitted by the biotin-streptavidin bond was still generated at the cell rear margin in the integrin-independent migration. The line profile of map was analyzed on the region marked by the yellow rectangle in (B). Line profile was obtained by averaging the rows of the rectangular region.

## DISCUSSION

By calibrating and mapping integrin molecular tension in migrating keratocytes at submicron resolution, we provided direct evidence to show that keratocytes mechanically mediate cell rear de-adhesion during rapid migration. We found that keratocytes produce HIT capable of rupturing integrin-ligand bonds exclusively and narrowly at the cell rear margin. HIT mediates rear de-adhesion by peeling off FAs lagging

behind during cell migration. The intensity of local HIT is highly correlated with cell retraction dynamics, showing that HIT promotes cell rear retraction and facilitates cell migration. HIT is also generated at the cell margin during artificially induced cell front retraction and during keratocyte migration mediated by actin-streptavidin bonds, suggesting that concentrating HIT at the cell margin is a general mechanism to mediate de-adhesion and retraction during keratocyte migration.

The narrow and exclusive localization of HIT at the cell margin raises the question of what is the direct force source of HIT because integrins are located in the cell membrane and linked to actin-based cytoskeleton. Cell membrane and cytoskeleton are the two potential physical sources for HIT. Actomyosin has been generally considered to be the main source of cell traction force produced at the cell-matrix interface (Lauffenburger and Horwitz, 1996; Ridley et al., 2003). However, it is doubtful that actomyosin is the direct force source for HIT that mediates keratocyte retraction. First, it is known that actomyosin is dispensable in keratocyte migration, as the pharmaceutical inhibition of actomyosin function does not prohibit keratocytes from migrating (Wilson et al., 2010). Moreover, if actomyosin generates HIT in migrating keratocytes, it is puzzling how actomyosin contraction may exclusively concentrate HIT at the cell rear margin within a narrow region of submicron width. A more plausible mechanism is that cell membrane instead of actomyosin generates HIT in rapidly migrating keratocytes. According to the actin treadmill model (Le Clainche and Carlier, 2008; Theriot and Mitchison, 1991), polymerizing actin network in cell protrusion site pushes the cell membrane forward, therefore stretching the cell membrane and producing a pulling force at the cell trailing edge (Lieber et al., 2013). HIT is likely generated on cell rear adhesion sites by tensioned cell membrane. This would explain why HIT is concentrated in a narrow region and consistently produced at the cell rear margin. This hypothesis is also favorably supported by the experiments of acute membrane retraction induced by osmotic shock during which HIT was generated at the cell margin in all peripheral locations, including the cell front, as the osmotic shock acutely induces membrane retraction but unlikely has an immediate effect on actomyosin force alteration. The biotin-streptavidin-based keratocyte migration also favorably supports the hypothesis that the cell membrane is the force source of HIT. It was shown that biotinylated keratocytes were able to adhere and migrate on streptavidin-presenting surface via biotin-streptavidin bonds. ITS signal reporting high-level tension was still generated at the cell rear margin in this integrin-independent keratocyte migration. Because actomyosin is not physically linked with most membrane proteins, the ITS signal was more likely generated by the cell membrane.

Nonetheless, it is challenging to rigorously rule out the role of actomyosin in the generation of HIT. We attempted to pharmaceutically inhibit myosin II in keratocytes using blebbistatin and indeed observed that HIT signal gradually diminished (Figures S4A and S4B). However, this does not suggest that actomyosin is the direct source of HIT. Because blebbistatin has the side effect of abolishing FA formation (Figure S4C) and weakening cell adhesion (Jurado et al., 2005), the decrease of HIT could simply be caused by the FA abolishment as HIT is generated to peel off FAs. In the future, an approach that inhibits myosin II while preserving FA formation is desired to confirm that actomyosin is not involved in HIT generation in migrating keratocytes.

Overall, our results provide the solid evidence that fast migrating keratocytes mechanically mediate cell rear de-adhesion by concentrating HIT exclusively at the cell rear margin to rupture the integrin-ligand bonds, testifying that mechanical regulation plays an important role in rapid cell migration.

### Limitations of the Study

This study was based on keratocytes as the cell models. Keratocytes are one rare type of cells that migrate rapidly at a rate comparable with that of neutrophils but still form strong FA sites. This study revealed the biomechanical mechanism that keratocytes concentrate HIT to efficiently detach the FAs during rapid migration. However, most other migratory metazoan cells migrate at much lower rates, typically 1%–10% of the rate of keratocytes. The conclusion drawn in this manuscript based on keratocytes may not be applicable to those cells with lower motility. The mechanism for cell de-adhesion in more common migratory cells awaits further investigation.

### METHODS

All methods can be found in the accompanying [Transparent Methods supplemental file](#).

## SUPPLEMENTAL INFORMATION

Supplemental Information includes Transparent Methods, four figures, and five videos and can be found with this article online at <https://doi.org/10.1016/j.isci.2018.11.016>.

## ACKNOWLEDGMENTS

This work was supported by the startup fund provided by Iowa State University. This work was also supported by National Institutes of Health (1R35GM128747).

## AUTHOR CONTRIBUTIONS

X.W. conceived the idea. Y.Z., Y.W., A.S., and X.W. designed and performed the experiments. X.W. and Y.Z. wrote the MATLAB code and analyzed the data. X.W. wrote the manuscript. All authors discussed the results and commented on the manuscript.

## DECLARATION OF INTERESTS

The authors declare that they have no conflict of interest.

Received: July 9, 2018

Revised: August 30, 2018

Accepted: November 7, 2018

Published: November 30, 2018

## REFERENCES

- Barnhart, E.L., Allen, G.M., Julicher, F., and Theriot, J.A. (2010). Bipedal locomotion in crawling cells. *Biophys. J.* **98**, 933–942.
- Carragher, N.O., and Frame, M.C. (2004). Focal adhesion and actin dynamics: a place where kinases and proteases meet to promote invasion. *Trends Cell Biol.* **14**, 241–249.
- Crisalli, P., and Kool, E.T. (2011). Multi-path quenchers: efficient quenching of common fluorophores. *Bioconjugate Chem.* **22**, 2345–2354.
- Even-Ram, S., Doyle, A.D., Conti, M.A., Matsumoto, K., Adelstein, R.S., and Yamada, K.M. (2007). Myosin IIA regulates cell motility and actomyosin microtubule crosstalk. *Nat. Cell Biol.* **9**, 299–309.
- Franco, S.J., and Huttenlocher, A. (2005). Regulating cell migration: calpains make the cut. *J. Cell Sci.* **118**, 3829–3838.
- Galior, K., Liu, Y., Yehl, K., Vivek, S., and Salaita, K. (2016). Titin-based nanoparticle tension sensors map high-magnitude integrin forces within focal adhesions. *Nano Lett.* **16**, 341–348.
- Gardel, M.L., Schneider, I.C., Aratyn-Schaus, Y., and Waterman, C.M. (2010). Mechanical integration of actin and adhesion dynamics in cell migration. *Annu. Rev. Cell Dev. Biol.* **26**, 315–333.
- Hatch, K., Danilowicz, C., Coljee, V., and Prentiss, M. (2008). Demonstration that the shear force required to separate short double-stranded DNA does not increase significantly with sequence length for sequences longer than 25 base pairs. *Phys. Rev. E Stat. Nonlin. Soft Matter Phys.* **78**(1 Pt 1), 011920.
- Houk, A.R., Jilkine, A., Mejean, C.O., Boltyanskiy, R., Dufresne, E.R., Angenent, S.B., Altschuler, S.J., Wu, L.F., and Weiner, O.D. (2012). Membrane tension maintains cell polarity by confining signals to the leading edge during neutrophil migration. *Cell* **148**, 175–188.
- Huttenlocher, A., and Horwitz, A.R. (2011). Integrins in cell migration. *Cold Spring Harb. Perspect. Biol.* **3**, a005074.
- Jurado, C., Haserick, J.R., and Lee, J. (2005). Slipping or gripping? Fluorescent speckle microscopy in fish keratocytes reveals two different mechanisms for generating a retrograde flow of actin. *Mol. Cell Biol.* **16**, 507–518.
- Jurchenko, C., Chang, Y., Narui, Y., Zhang, Y., and Salaita, K.S. (2014). Integrin-generated forces lead to streptavidin-biotin unbinding in cellular adhesions. *Biophys. J.* **106**, 1436–1446.
- Kong, F., Garcia, A.J., Mould, A.P., Humphries, M.J., and Zhu, C. (2009). Demonstration of catch bonds between an integrin and its ligand. *J. Cell Biol.* **185**, 1275–1284.
- Lamallice, L., Le Boeuf, F., and Huot, J. (2007). Endothelial cell migration during angiogenesis. *Circ. Res.* **100**, 782–794.
- Lauffenburger, D.A., and Horwitz, A.F. (1996). Cell migration: a physically integrated molecular process. *Cell* **84**, 359–369.
- Le Clairche, C., and Carlier, M.F. (2008). Regulation of actin assembly associated with protrusion and adhesion in cell migration. *Physiol. Rev.* **88**, 489–513.
- Lee, J., Ishihara, A., Oxford, G., Johnson, B., and Jacobson, K. (1999). Regulation of cell movement is mediated by stretch-activated calcium channels. *Nature* **400**, 382–386.
- Lieber, A.D., Yehudai-Resheff, S., Barnhart, E.L., Theriot, J.A., and Keren, K. (2013). Membrane tension in rapidly moving cells is determined by cytoskeletal forces. *Curr. Biol.* **23**, 1409–1417.
- Liu, Y., Medda, R., Liu, Z., Galior, K., Yehl, K., Spatz, J.P., Cavalcanti-Adam, E.A., and Salaita, K. (2014). Nanoparticle tension probes patterned at the nanoscale: impact of integrin clustering on force transmission. *Nano Lett.* **14**, 5539–5546.
- Liu, Y., Yehl, K., Narui, Y., and Salaita, K. (2013). Tension sensing nanoparticles for mechanomicroimaging at the living/nonliving interface. *J. Am. Chem. Soc.* **135**, 5320–5323.
- Luster, A.D., Alon, R., and von Andrian, U.H. (2005). Immune cell migration in inflammation: present and future therapeutic targets. *Nat. Immunol.* **6**, 1182–1190.
- Maiuri, P., Terriac, E., Paul-Gilloteaux, P., Vignaud, T., McNally, K., Onuffer, J., Thorn, K., Nguyen, P.A., Georgoulia, N., Soong, D., et al. (2012). The first world cell race. *Curr. Biol.* **22**, R673–R675.
- Mondal, G., Barui, S., and Chaudhuri, A. (2013). The relationship between the cyclic-RGDfK ligand and alpha v beta 3 integrin receptor. *Biomaterials* **34**, 6249–6260.
- Murrell, M., Oakes, P.W., Lenz, M., and Gardel, M.L. (2015). Forcing cells into shape: the mechanics of actomyosin contractility. *Nat. Rev. Mol. Cell Biol.* **16**, 486–498.
- Palecek, S.P., Huttenlocher, A., Horwitz, A.F., and Lauffenburger, D.A. (1998). Physical and biochemical regulation of integrin release during rear detachment of migrating cells. *J. Cell Sci.* **111**, 929–940.
- Pincet, F., and Husson, J. (2005). The solution to the streptavidin-biotin paradox: the influence of history on the strength of single molecular bonds. *Biophys. J.* **89**, 4374–4381.

Pollard, T.D., and Borisy, G.G. (2003). Cellular motility driven by assembly and disassembly of actin filaments. *Cell* 112, 453–465.

Poujade, M., Grasland-Mongrain, E., Hertzog, A., Jouanneau, J., Chavrier, P., Ladoux, B., Buguin, A., and Silberzan, P. (2007). Collective migration of an epithelial monolayer in response to a model wound. *Proc. Natl. Acad. Sci. U S A* 104, 15988–15993.

Riaz, M., Versaevel, M., Mohammed, D., Glinel, K., and Gabriele, S. (2016). Persistence of fan-shaped keratocytes is a matrix-rigidity-dependent mechanism that requires alpha(5) beta(1) integrin engagement. *Sci. Rep.* 6, 34141.

Ridley, A.J., Schwartz, M.A., Burridge, K., Firtel, R.A., Ginsberg, M.H., Borisy, G., Parsons, J.T., and Horwitz, A.R. (2003). Cell migration: integrating signals from front to back. *Science* 302, 1704–1709.

Sheetz, M.P., Felsenfeld, D.P., and Galbraith, C.G. (1998). Cell migration: regulation of force on

extracellular-matrix-integrin complexes. *Trends Cell Biol.* 8, 51–54.

Theriot, J.A., and Mitchison, T.J. (1991). Actin microfilament dynamics in locomoting cells. *Nature* 352, 126–131.

Undyala, V.V., Dembo, M., Cembrola, K., Perrin, B.J., Huttenlocher, A., Elce, J.S., Greer, P.A., Wang, Y.L., and Beningo, K.A. (2008). The calpain small subunit regulates cell-substrate mechanical interactions during fibroblast migration. *J. Cell Sci.* 121, 3581–3588.

Wang, X.F., and Ha, T. (2013). Defining single molecular forces required to activate integrin and Notch signaling. *Science* 340, 991–994.

Wang, X.F., Sun, J., Xu, Q., Chowdhury, F., Rooin-Peikar, M., Wang, Y.X., and Ha, T. (2015). Integrin molecular tension within motile focal adhesions. *Biophys. J.* 109, 2259–2267.

Wang, Y., LeVine, D.N., Gannon, M., Zhao, Y., Sarkar, A., Hoch, B., and Wang, X. (2017). Force-activatable biosensor enables single platelet

force mapping directly by fluorescence imaging. *Biosens. Bioelectron.* 100, 192–200.

Wang, Y., and Wang, X. (2016). Integrins outside focal adhesions transmit tensions during stable cell adhesion. *Sci. Rep.* 6, 36959.

Weijer, C.J. (2009). Collective cell migration in development. *J. Cell Sci.* 122, 3215–3223.

Weyand, B., Warth, R., Bleich, M., Kerstan, D., Nitschke, R., and Greger, R. (1998). Hypertonic cell shrinkage reduces the K<sup>+</sup> conductance of rat colonic crypts. *Pflugers Arch.* 436, 227–232.

Wilson, C.A., Tsuchida, M.A., Allen, G.M., Barnhart, E.L., Applegate, K.T., Yam, P.T., Ji, L., Keren, K., Danuser, G., and Theriot, J.A. (2010). Myosin II contributes to cell-scale actin network treadmill through network disassembly. *Nature* 465, 373–377.

Yilmaz, M., and Christofori, G. (2010). Mechanisms of motility in metastasizing cells. *Mol. Cancer Res.* 8, 629–642.

**ISCI, Volume 9**

**Supplemental Information**

**Keratocytes Generate High Integrin**

**Tension at the Trailing Edge to Mediate**

**Rear De-adhesion during Rapid Cell Migration**

**Yuanchang Zhao, Yongliang Wang, Anwesha Sarkar, and Xuefeng Wang**

## Supplemental Information

### **Keratocytes generate high-level integrin tension at the trailing edge to mediate rear de-adhesion during rapid cell migration**

Yuanchang Zhao<sup>1</sup>, Yongliang Wang<sup>1</sup>, Anwesha Sarkar<sup>1</sup> and Xuefeng Wang<sup>1,2,3,\*</sup>

<sup>1</sup>Department of Physics and Astronomy, Iowa State University, 12 Physics Hall, Ames, IA 50011, USA.

<sup>2</sup>Molecular, Cellular, and Developmental Biology interdepartmental program, Molecular Biology Building, Ames, IA 50011, USA.

<sup>3</sup>Lead Contact

\*Correspondence: [xuefeng@iastate.edu](mailto:xuefeng@iastate.edu)

## Supplementary Figures

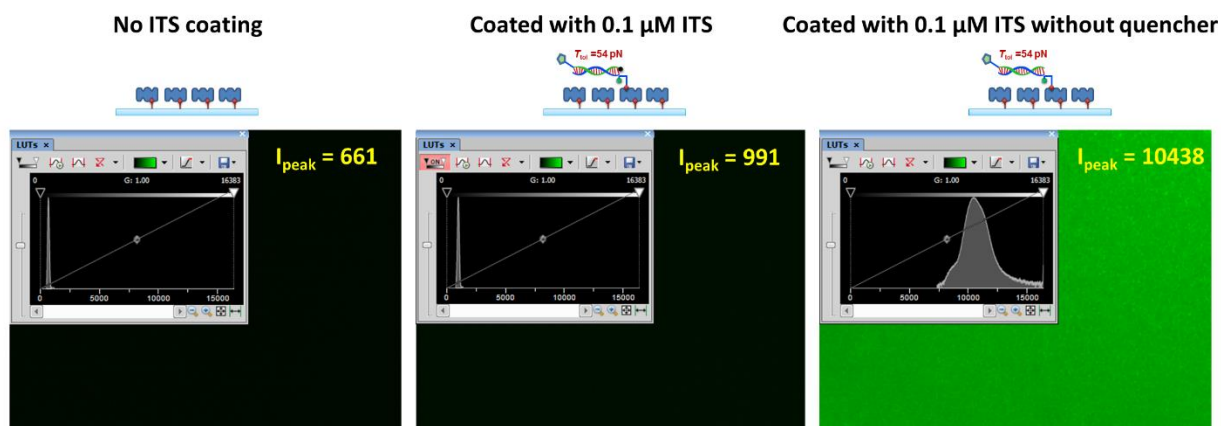


**Figure S1. Calibration of quenching efficiency of Cy3-quencher pair in ITS, Related to Figure 1.** Under the same imaging setting, we acquired fluorescence intensities on neutravidin-coated glass surfaces without ITS coating, with 0.1  $\mu\text{M}$  ITS coating, and with 0.1  $\mu\text{M}$  quencher-free ITS coating, respectively. The average grayscale values (denoted by  $I_{\text{peak}}$ , the grayscale value at the peak of grayscale histogram) represent the fluorescence intensities on these surfaces, from which the quenching efficiency of Cy3-quencher pair in 54 pN ITS was calculated as:  $(10438-991)/(10438-661)=96.6\%$ .

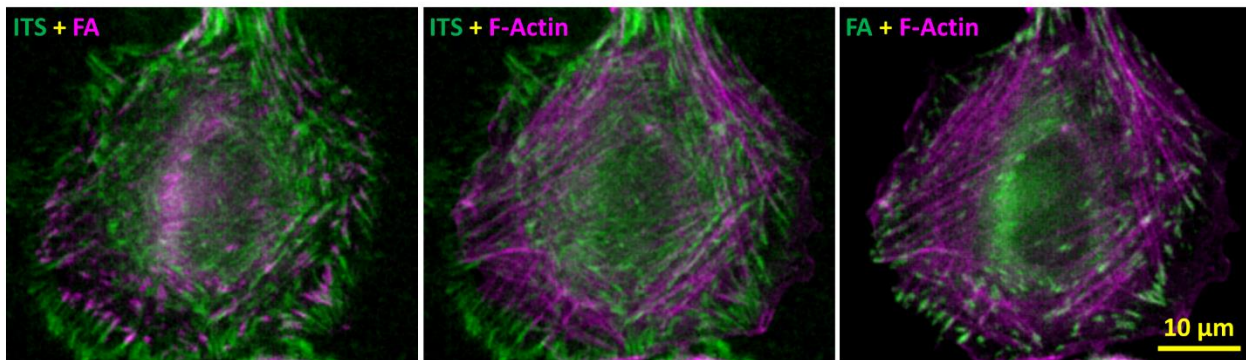


**Figure S2. Merged images of focal adhesions (FA), F-actin and ITS signal ( $T_{\text{tot}} = 54$  pN) in a CHO-K1 cell, Related to Figure 3.** Two images instead of three selected from FA, F-actin and ITS imaging were merged to show the local connection between ITS and cellular structures with better clarity.

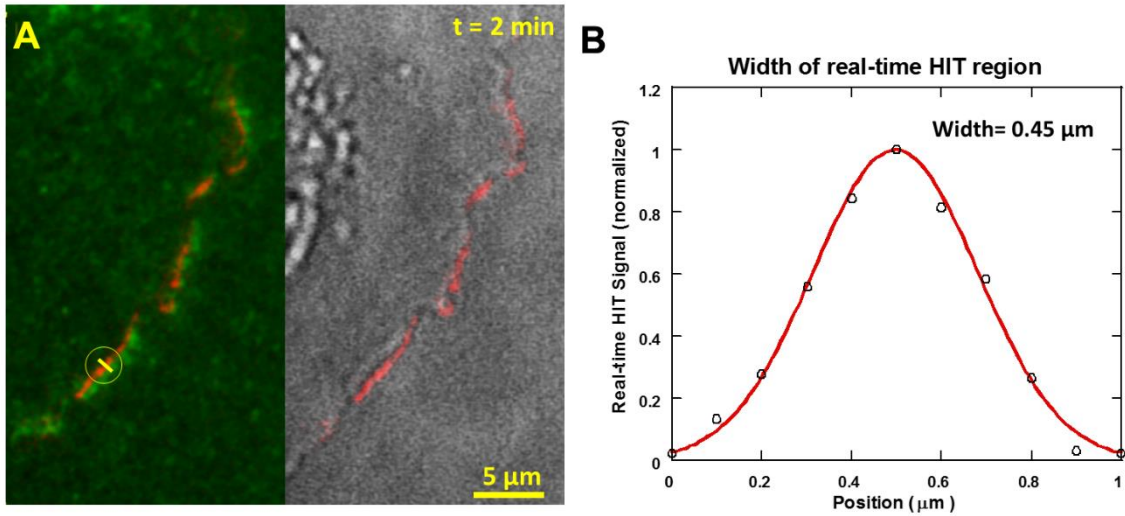


**Figure S3. Width calibration of real-time HIT region during acutely induced cell front retraction, Related to Figure 5.**

**A** HIT map (green), real-time HIT map generated in latest 10 seconds (red) and the cell margin.

**B** The width of real-time HIT region is calibrated to be 0.45  $\mu\text{m}$ . The line profile was analyzed based on the circled region in **A**. The HIT signal was represented by the grayscale value of pixels along the yellow line in the yellow circle.

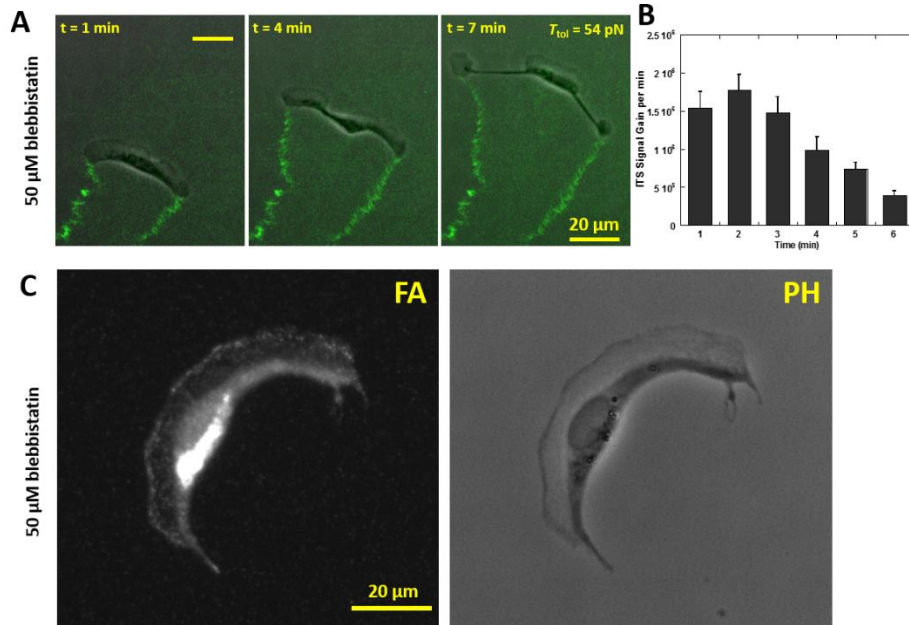


**Figure S4. HIT diminished in keratocytes treated with 50  $\mu$ M blebbistatin that abolishes focal adhesion formation, Related to Figure 5.**

- A** A keratocyte continued to migrate with myosin II inhibited by 50  $\mu$ M blebbistatin.
- B** HIT reported by ITS signal decreased by time.
- C** Focal adhesions were abolished by the treatment of 50  $\mu$ M blebbistatin, likely resulting in the HIT diminishing as HIT is generated to peel off focal adhesions.

## Transparent Methods

Buffer solutions for all reactions in the methods are PBS (phosphate buffered saline) with PH=7.4 if not stated otherwise.

**Synthesis of ITS.** ITS is synthesized based on a double-stranded DNA (dsDNA). The dsDNA is decorated with four molecular tags as shown in Fig. 1b. Only the upper strand of dsDNA requires integrin ligand conjugation. All other DNA strands with modifications can be customized and purchased from commercial sources. The upper strand DNA with thiol modification and BHQ2 (black hole quencher 2) tag was purchased from integrated DNA technology, Inc. Integrin ligand peptide RGD was conjugated on this ssDNA at 5' end with the following protocol.

Sequence and modification of the upper strand ssDNA of ITS:

5'- /5ThioMC6-D/GGG CGG CGA CCT CAG CAT/3BHQ2/ -3'

### Conjugation of RGD peptide on thiol-modified ssDNA.

1). 20 $\mu$ L $\times$ 1 mM ssDNA with thiol modification was mixed with 10  $\mu$ L $\times$ [50mM TCEP + 50mM EDTA] and incubated at room temperature for 30 min. TCEP and EDTA were used to deprotect the thiol group and make it available for thiol-maleimide reaction. TCEP: Tris(2-carboxyethyl)phosphine hydrochloride. EDTA: Ethylenediaminetetraacetic acid. 2). Mix 100  $\mu$ L $\times$ 20 mM Cyclic peptide RGD-NH<sub>2</sub> (catalog #: PCI-3696-PI, purchased from Peptides International Inc) and 40  $\mu$ L $\times$ 23mM Sulfo-SMCC (crosslinker with NHS ester and Maleimide groups, 22622, Thermo Fisher Scientific Inc.) dissolved in pure water, and incubate the mixture for 20 min at room temperature. The NHS ester group on the Sulfo-SMCC crosslinker reacts with the amine on RGD, while maleimide at the other end of the crosslinker is saved for the reaction with thiol group on the thiol-modified ssDNA in the next step. 3). The solutions of ssDNA with thiol group and RGD linked to crosslinker were mixed and kept at room temperature for 1 h and then at 4 °C overnight. RGD-maleimide reacts with thiol-ssDNA and form the product of RGD-ssDNA-BHQ2. The ssDNA was purified by ethanol precipitation. This protocol generally have more than 80% yield of RGD-ssDNA-BHQ2. If higher purity is desired, the ssDNA can be further purified by gel electrophoresis or HPLC.

RGD-ssDNA-BHQ2 was hybridized with its complementary ssDNA with fluorophore and biotin tags to form the final product of ITS. The hybridization is performed by mixing RGD-ssDNA-BHQ2 and Fluor-ssDNA-biotin at 1.2:1 molar ratio and incubating the mixture at 4 °C overnight. Although both ssDNA with conjugates can tolerate temperature for standard DNA annealing, it is not necessary to anneal the two ssDNAs at high temperature as these 18bp ssDNAs were designed to have minimized secondary structure. The following shows the DNA structure for ITS used in this paper. "BiosG" and "Bio" denote biotin conjugation on the ssDNA.

ITS with  $T_{\text{tot}} = 54$  pN (with Cy3-BHQ2 pair)

5'- /5RGD/-GGG CGG CGA CCT CAG CAT/3BHQ2/ -3'

5'- /5BiosG/T/iCy3/ATG CTG AGG TCG CCG CCC/ -3'

ITS with  $T_{\text{tot}} = 100$  pN (with Cy3 label and reporting integrin tensions by fluorescence loss)

5'- /5RGD/-GGG CGG CGA CCT CAG CAT/3Bio/ -3'

5'- ATG CTG AGG TCG CCG CCC/Cy3/ -3'

ITS with  $T_{\text{tot}} = 54$  pN (with Cy3 label and reporting integrin tensions by fluorescence loss)

5'- /5RGD/-GGG CGG CGA CCT CAG CAT/Cy3/ -3'

5'- /5BiosG/ATG CTG AGG TCG CCG CCC/ -3'

**ITS surface preparation.** ITS is immobilized on a glass surface through biotin-streptavidin interaction. 1). 0.5 mg/mL biotinylated bovine serum albumin (BSA-biotin, Prod #: 29130, purchased from ThermoFisher Scientific Inc) was incubated on a glass-bottom petri dish (D35-10-1.5-N, Cellvis) at 4 °C for 30 min and the surface was thoroughly washed by PBS three times. 2). 100 µg/mL streptavidin (S4762, Sigma-Aldrich) was added to the surface and incubated at 4 °C for 30 min. The petri dish was rinsed with PBS solution three times. 3). 0.1 µM ITS solution was added on the streptavidin coated surface and incubated at 4 °C for 30 min. The surface was rinsed with PBS three times and kept in PBS before cell plating.

**Cell culture and plating.** The keratocytes were harvested from scales of fantail goldfish (*Carassius auratus*). Fish scales were plucked from a fish and gently pressed on a glass bottom petri dish, with the interior side of the scale contacting on the glass surface. Allow 1-2 min for the scale to stick on the surface. Then add culture medium (IMDM, Lot #:62996227, purchased from ATCC company) spiked with 20% fetal bovine serum and 1% penicillin on the petri dish. The scales were incubated at room temperature for about 12-24 h to allow keratocytes to migrate out from the scales.

In experiments, the keratocytes were detached from petri dish using EDTA solution (Recipe: 100mL 10× HBSS + 10mL 1M HEPES (PH7.6) + 10 mL 7.5% sodium bicarbonate + 2.4 mL 500 mM EDTA +1 L H<sub>2</sub>O). The petri dish with keratocytes was rinsed once with EDTA solution and then incubated in the EDTA solution for 5 min at room temperature. The detached cells were dispersed in the EDTA solution by pipetting. IMDM culture medium was added to the EDTA solution with cells at a volume ratio of 5:1. The keratocytes were plated on the ITS surface at a cell density of 2.0×10<sup>5</sup> cells/mL in the well of the petri dish. This relatively low cell density allows more space for cell migration. Incubate the cells on ITS surface for about 15 min. Keratocytes will polarize and migrate. The ITS imaging is performed afterwards. Experiments with goldfish were under supervision of IACUC (Institutional Animal Care and Use Committee. Log number: 8-16-8333-I).

#### **Mn<sup>2+</sup> treatment on migrating keratocytes**

Name: Magnesium Chloride Hexahydrate

Company: Fisher Scientific

Concentration: 2mM

When keratocytes were migrating on the ITS surface, 1 mL cell medium spiked with 2.4 mM MnCl<sub>2</sub> (bp214-500, Fisher Scientific) was added to the petridish well which contains keratocytes in 200 µL medium. The final concentration of Mn<sup>2+</sup> is 2 mM.

**FA (focal adhesion) immunostaining.** Immunostaining of FA protein vinculin was performed to visualize FAs and study their co-localization with ITS maps using standard immunostaining protocol. 2.5 µg/mL primary antibody (Vinculin Monoclonal antibody, purified clone 7F9 (Part No. 90227), purchased from Millipore Sigma), 2.5 µg/mL secondary antibody (mouse anti-human CD62P, Catalog No. 550561, purchased from BD Boisciences) and 2 unit/mL phalloidin (Alexa Fluor® 647 Phalloidin , Catalog No. A22287, purchased from ThermoFisher Scientific Inc) was used to stain vinculin and F-actin.

#### **Experiments with treatment of hypertonic medium, blebbistatin, Y-27362 and Calpain inhibitor.**

All inhibition experiments were conducted on live migrating keratocytes. The petri dish coated with ITS and plated with keratocytes was mounted on the stage in the fluorescence microscope. Hypertonic medium was added by medium exchange after cell adhesion. Blebbistatin, Y-27632 or Calpain inhibitor was added to cell medium prior to cell plating and remained in the medium during the entire experiments.

#### **Biotinylation of keratocytes.**

Keratocytes in culture was treated with 0.5mM EZ-Link™ NHS-PEG12-Biotin (21312, ThermoFisher Scientific) in Ham's F12 (HFL05 , Caisson Lab, Inc.) medium (without fetal bovine serum) for 10 min.

The cells were then rinsed with Ham's F12 medium twice, detached by EDTA solution and prepared for subsequent migration experiments.

**Imaging acquisition.** Imaging on keratocytes was performed at room temperature using Nikon Eclipse Ti-E fluorescence microscope with 40× and 1.5× tube lens. ITS with  $T_{\text{tot}} = 54$  pN was imaged in Cy3 channel. YFP channel was used to image immunostained vinculin for FA visualization. Software NIS elements was used to control the microscope and image acquisition.

**Image analysis.** Matlab code was compiled for the image analysis and video processing. All ITS signal intensities were acquired from the original fluorescence images without rescaling of image grayscale. Matlab code was also compiled to find cell contours, the code is available upon request.